Bull. Mater. Sci. (2020) 43:54
https://doi.org/10.1007/s12034-019-2011-1

Temperature-dependence calculation of lattice thermal conductivity and related parameters for the zinc blende and wurtzite structures of InAs nanowires

HAWBASH H KARIM[1,*] and M S OMAR[2]
[1]Department of Physics, Faculty of Science and Health, Koya University, 44023 Koya, Kurdistan Region-F.R., Iraq
[2]Department of Physics, College of Science, Salahaddin University – Erbil, Erbil, Kurdistan Region, Iraq
*Author for correspondence (Hawbash.hamadamin@koyauniversity.org)

MS received 9 April 2019; accepted 24 October 2019

Abstract. Theoretical calculations are performed on lattice thermal conductivity (LTC) and related parameters for the zinc blende and wurtzite structure of InAs nanowires (NWs) with diameters of 50, 63, 66, 100 and 148 nm through the Morelli–Callaway model. For the model to be efficiently applicable, the longitudinal and transverse modes are considered. The melting point of the various-sized NWs is considered to estimate the Debye and phonon group velocities. The impacts of Grüneisen parameter, dislocations and surface roughness are also successfully utilized to address the calculated and measured LTC of the semiconductor under investigation. Results show that the Grüneisen parameter increases with decreasing NW diameter and that phonon confinement leads to an observable deviation of the calculated LTC curve from that of the experimental one in the case of bulk InAs. We assume that NW boundaries, dislocations and imperfections are responsible for the scattering of phonons along with electrons and other phonons because of normal and Umklapp processes. Therefore, at a specified temperature, LTC depends on the size and crystal structure of the semiconductor. As such, the thermal and mechanical parameters of InAs can be greatly modified by decreasing the size and dimension of the semiconductor as a result of the quantum-confinement effect.

Keywords. Lattice thermal conductivity; InAs nanowire; phonon scatterings; morelli–Callaway model; grüneisen parameter.

1. Introduction

One of the most important physical parameters of materials is thermal conductivity owing to its wide utilization in technical applications, such as thermal management of nuclear, electrical, mechanical and chemical systems. Thermal conductivity can also be considered in materials that can behave as thermal barriers and thermal insulators. Thermoelectric semiconductors also have applications in diode lasers and infrared sensors [1]. One-dimensional semiconductor nanowires (NWs), in the range of a few to several tens of nanometers, are potential next-generation building blocks for nanoscale electronics, photonics, sensors and lasers.

The main factor to reduce heat flow in semiconductors is defect. Its concentration increases with the reduction of NW diameter, which in turn reduces the value of lattice thermal conductivity (LTC) dramatically, similar to that reported elsewhere [2,3]. However, Estreicher *et al* [4] showed that thermal phonons can be trapped by spatially localized vibrational modes (SLMs), while Cahill *et al* [5] claimed that there exist some other parameters that affect LTC, including grain size, doping and point defects, anisotropic crystals and natural superlattices.

Indium arsenide (InAs) NWs are of particular interest for their excellent electron-transport property and remarkably high electron mobility owing to their small effective mass. Thermodynamic parameters play important roles in structural phase change, which has a large effect on physical properties [6]. InAs crystallizes under normal conditions and typically presents itself in a cubic zinc blende (ZB) structure [7,8]. Bulk InAs has a cubic ZB structure with lattice constant $a = 6.058$ Å and melting point of 1216 K. InAs has a small band gap of 0.354 eV and its intrinsic carrier concentration reaches about 1.15×10^{15} cm^{-3} [9].

In the present work, the LTCs of wurtzite (WZ) and ZB InAs NWs are measured theoretically using a Callaway expression, and results are fitted with experimental data as reported in refs. [10] and [11], respectively. The Callaway expression for phonon conductivity (including the three mechanisms), the effect of dislocation, phonon–electron, boundary, phonon–phonon Umklapp and normal three-phonon scattering are used to calculate LTC in each of the aforementioned cases. Many size-dependent parameters such as mean free path, lattice constant, unit-cell volume, melting temperature, Debye temperature and acoustic group velocity are calculated. Some parameters such as dislocation density, impurity, carrier

Published online: 24 January 2020

concentration, surface roughness and Grüneisen parameter for both longitudinal and transverse modes are used to fit the theoretical curve to that of the experimental counterparts [12].

2. Theory and calculations

The structure and atomic distribution of InAs are well known due to their widely experimental investigation in literature [13]. Its cubic ZB structure form has a lattice constant $a = 6.058$ Å. The Morelli–Callaway model [14], which is a modification of last version of Callaway model [15], is applied to calculate LTC as a function of temperature for some binary compounds.

2.1 *General formalism for the LTC*

The approach used by Asen-Palmer *et al* [16], was considered to calculate the LTC as follows [14]:

$$\kappa = AT^3 \int_0^{\theta_D/T} \tau_c J(x) dx \tag{1}$$

where $A = (k_B/\hbar)^3 (k_B/(2\pi^2 v))$, $J(x) = x^4 e^x (e^x - 1)^{-2}$, $x = \hbar\omega/k_B T$, k_B is the Boltzmann constant (1.38065×10^{-23} m^2 kg s^{-2} K^{-1}), $\hbar$ is Planck's constant (1.05457×10^{-23} J s), τ_c is the phonon-relaxation time, θ_D is the Debye temperature, v is the acoustic group velocity, ω is the phonon angular frequency and T is the absolute temperature in Kelvin. Equation (1) can enable good theoretical calculation of LTC for thin films and NWs [17,18]. This model has been modified to the Debye–Callaway formalism and summed over one longitudinal (k_L) and two degenerate transverse (k_T) phonon branches [14]:

$$\kappa = \kappa_L + 2\kappa_T, \tag{2}$$

$$\kappa_L = \kappa_{L_1} + \kappa_{L_2}, \tag{2a}$$

$$\kappa_T = \kappa_{T_1} + \kappa_{T_2}. \tag{2b}$$

In equation (2a), κ_{L_1} and κ_{L_2} are the usual Debye–Callaway terms expressed as follows:

$$\kappa_{L_1} = \frac{1}{3} A_L T^3 \int_0^{\theta_D^L/T} \tau_c^L(x) J(x) dx, \tag{3}$$

$$\kappa_{L_2} = \frac{1}{3} A_L T^3 \left[\int_0^{\theta_D^L/T} \frac{\tau_c^L(x)}{\tau_N^L(x)} J(x) dx \right]^2 \times \left[\int_0^{\theta_D^L/T} \frac{\tau_c^L(x)}{\tau_N^L(x)\tau_R^L(x)} J(x) dx \right]^{-1}. \tag{4}$$

Similarly, for the transverse phonons, they are expressed by [3,19]

$$\kappa_{T_1} = \frac{1}{3} A_T T^3 \int_0^{\theta_D^T/T} \tau_c^T(x) J(x) dx, \tag{5}$$

$$\kappa_{T_2} = \frac{1}{3} A_T T^3 \left[\int_0^{\theta_D^T/T} \frac{\tau_c^T(x)}{\tau_N^T(x)} J(x) dx \right]^2 \times \left[\int_0^{\theta_D^T/T} \frac{\tau_c^T(x)}{\tau_N^T(x)\tau_R^T(x)} J(x) dx \right]^{-1}, \tag{6}$$

where T and L denote longitudinal and transverse phonons, respectively. Moreover, θ_D^T and θ_D^L are the transverse and longitudinal Debye temperatures, respectively, and can be calculated as [14]

$$\theta_D^{L(T)} = \left(\frac{\omega_{L(T)} \pi^2}{V} \right)^{1/3} \frac{\hbar v_{L(T)}}{k_B} \tag{7}$$

where $\omega_{L(T)}$ is the longitudinal (transverse) phonon frequency, and $v_{L(T)}$ is the acoustic group velocity [20]. Furthermore, A_L in equation (4) and A_T in equation (6) are given as follows [21]:

$$A_L = \left(\frac{k_B}{\hbar} \right)^3 \frac{k_B}{2\pi^2 v_L}, \tag{8a}$$

$$A_T = \left(\frac{k_B}{\hbar} \right)^3 \frac{k_B}{2\pi^2 v_T}. \tag{8b}$$

2.2 *Phonon-scattering rates and Debye temperature for semiconductors*

The following expression is used to study various phonon-relaxation times and phonons affected by different scattering processes, including inharmonic interaction, phonon–phonon (normal three-phonon scattering $\tau_N^{L(T)}$ and Umklapp three-phonon scattering $\tau_U^{L(T)}$), phonon–impurity, $\tau_M^{L(T)}$, phonon–electron scattering, $\tau_{ph-e}^{L(T)}$, phonon–boundary, $\tau_B^{L(T)}$, and phonon–dislocation rate $\tau_{DC}^{L(T)}$. The different scattering process combinations of relaxation times can be expressed as [22]

$$\left(\frac{1}{\tau_C^{L(T)}} \right) = \left(\frac{1}{\tau_N^{L(T)}} \right) + \left(\frac{1}{\tau_U^{L(T)}} \right) + \left(\frac{1}{\tau_M^{L(T)}} \right) + \left(\frac{1}{\tau_B^{L(T)}} \right) + \left(\frac{1}{\tau_{ph-e}^{L(T)}} \right) + \left(\frac{1}{\tau_{DC}^{L(T)}} \right). \tag{9}$$

2.2a *Three phonon–phonon Umklapp and normal scattering processes*: The phonon–phonon Umklapp processes should give rise to an exponential behaviour of the LTC at high temperatures, in which the total phonon wave vectors are not conserved except for changes induced by a reciprocal lattice vector. To fix the Umklapp scattering rate for longitudinal and

transverse phonons, we select the following relation [14]:

$$\left[\tau_{\mathrm{U}}^{\mathrm{L(T)}}\right]^{-1} = B_{\mathrm{U}}^{\mathrm{L(T)}}\left(\frac{k_{\mathrm{B}}}{\hbar}\right)^{2} x^{2}T^{3}e^{-\left(\theta_{\mathrm{D}}^{\mathrm{L(T)}}/3T\right)} \tag{10}$$

where

$$B_{\mathrm{U}}^{\mathrm{L(T)}} = \frac{\hbar\gamma_{\mathrm{L(T)}}^{2}}{Mv_{\mathrm{L(T)}}^{2}\theta_{\mathrm{D}}^{\mathrm{L(T)}}}.$$

Here M is the average mass of an atom in the crystal and $\gamma_{\mathrm{L(T)}}$ is the Grüneisen parameter, whose value can be extracted by fitting to the thermal conductivities of the crystals [23].

Meanwhile, normal phonon scattering has an important effect in determining the LTC peak. Thus, the Umklapp scattering rate depends on the transverse and longitudinal Debye temperatures, phonon velocities and Grüneisen parameters; hence, its value differs for different phonon modes. It is mathematically expressed as [24]

$$\left[\tau_{\mathrm{N}}^{\mathrm{L(T)}}\right]^{-1} = B_{\mathrm{N}}^{\mathrm{L(T)}}\omega^{2}T^{3} \tag{11}$$

with

$$B_{\mathrm{N}}^{\mathrm{L}} = \frac{k_{\mathrm{B}}^{3}v_{\mathrm{L}}^{2}V}{M\hbar^{3}v_{\mathrm{L}}^{5}} \quad \text{and} \quad B_{\mathrm{N}}^{\mathrm{T}} = \frac{k_{\mathrm{B}}^{4}v_{\mathrm{T}}^{2}V}{M\hbar^{3}v_{\mathrm{T}}^{5}}$$

where V is lattice volume and calculated for each case, as listed in table 1.

2.2b *Phonon–impurity scattering rate*: Density and elastic changes in materials caused by impurities result in phonon scattering because these changes produce local variations in sound velocity. However, point-defect scattering leads us to introduce a problem into theoretical estimations. For instance, the relaxation time of such scattering should vary as $1/\omega^{4}$, where ω is the phonon angular frequency. As such, low-frequency phonons are only slightly affected by point-defect scattering [25]. Klemens first provided calculations for the scattering rate of phonons by isolated defects, having a mass differing from that of the host in an otherwise perfect crystal. Mass-difference scattering is phonon scattering caused by differences in mass [14]. The relaxation rate for the mass-difference scattering is measured with the following equation [24]:

$$\left[\tau_{\mathrm{M}}^{\mathrm{L(T)}}\right]^{-1} = \left(I_{\mathrm{iso}}^{\mathrm{L(T)}} + I_{\mathrm{imp}}^{\mathrm{L(T)}}\right)\omega^{4} \tag{12}$$

where $I_{\mathrm{iso}}^{\mathrm{L(T)}}$ is phonon scattering due to different isotopes of an element or compound and can be calculated for each mode as follows:

$$I_{\mathrm{iso}}^{\mathrm{L(T)}} = \frac{V\Gamma}{4\pi v_{\mathrm{L(T)}}^{3}}.$$

Likewise, $I_{\mathrm{imp}}^{\mathrm{L(T)}}$ is the phonon-scattering distribution caused by impurity and is represented as

$$I_{\mathrm{imp}}^{\mathrm{L(T)}} = \frac{3V^{2}S^{2}}{\pi v_{\mathrm{L(T)}}^{3}}N_{\mathrm{imp}}$$

where S is the scattering factor, whose value is equal to one [21,26]. In addition, N_{imp} is the concentration of impurity, whose value can be found from the fitting of LTC curve. The general form of each element can be represented as

$$\Gamma = \sum\nolimits_{i} c_{i}\left(\frac{m_{i}-\bar{m}}{\bar{m}}\right)^{2} \tag{13}$$

where c_i is the percentage atomic natural abundance, m_i is the atomic mass of the i^{th} isotope and $\bar{m}$ is the average atomic mass ($\bar{m} = \sum_i c_i m_i$). The correct calculation of Γ for a binary compound, such as InAs composed of two different elements,

Table 1. Calculated diameter-dependence values for mean bonding length (equation (23)), lattice parameter (equation (25)), lattice volume (equation (26)), melting temperature (equation (27)), longitudinal and transverse Debye temperatures, NWs (equation (28)) and phonon group velocity for longitudinal and transverse NWs (equation (29)).

Diameter (nm)	Mean bonding length (Å)	Lattice constant (Å)	Lattice volume (Å^3)	Melting temperature T_{m} (K)	Debye temperature (K)		Group velocity (m s^{-1})	
					$\theta_{\mathrm{D}}^{\mathrm{L}}$	$\theta_{\mathrm{D}}^{\mathrm{T}}$	$v_{\mathrm{g}}^{\mathrm{L}}$	$v_{\mathrm{g}}^{\mathrm{T}}$
50	2.65614	6.1341	28.8511	1197.33	184.128	78.7714	4273.35	2067.75
63	2.653	6.12683	28.7487	1201.22	184.728	79.0279	4287.26	2074.48
66	2.65245	6.12557	28.7309	1201.9	184.832	79.0726	4289.69	2075.65
100	2.64854	6.11654	28.604	1206.73	185.575	79.3902	4306.92	2083.99
148	2.646609	6.11088	28.5247	1209.75	186.039	79.5889	4317.7	2089.21
Bulk	2.641	6.058	27.7906	1216	187	80	4340	2100

Table 2. Material parameters of InAs.

Name	Abbreviation	Value	Reference
Ideal gas constant	R	8.314 (J K^{-1} mol^{-1})	Ref. [30]
First surface layer height	h	0.3773989 (nm)	From Eq. (20)
Enthalpy of fusion	H_m		From Eq. (22)
Bulk overall melting entropy	$S_m(\infty)$	30.21 (J K^{-1} mol^{-1})	Ref. [30]
Mass per atom	M	$31.4967736 \times 10^{-26}$ (kg)	Ref. [31]
Strength of the mass-difference scattering	Γ	3.45×10^{-4}	Eq. (15)
Mean bond length	d_{mean}	0.2641 (nm)	Ref. [30]
Melting temperature	T_m	1216	Ref. [30]
Scattering factor	S	1	Ref. [26]
Indium isotopes	^{113}In, ^{115}In	4.330%, 95.67%	Ref. [32]
Arsenic isotopes	^{75}As	100%	Ref. [32]
Weight factor	η	0.55	Ref. [33]
Deformation potential	E_n	0.354 (eV)	Refs. [9,29]
Effective mass	m^*	$0.023m_e$	Ref. [7]
Electron rest mass	m_e	9.10938356 (kg)	Ref. [8]

is given as [14]

$$\Gamma(\mathrm{InAs})=2\left[\left(\frac{M_{\mathrm{In}}}{M_{\mathrm{In}}+M_{\mathrm{As}}}\right)^2\Gamma(\mathrm{In})+\left(\frac{M_{\mathrm{As}}}{M_{\mathrm{In}}+M_{\mathrm{As}}}\right)^2\Gamma(\mathrm{As})\right] \tag{14}$$

where M_{In} and M_{As} are the average atomic mass of In and As, respectively [14]. The strength for each of In and As isotopes is listed in table 2.

2.2c *Phonon–boundary scattering rate*: For nanostructures, an additional boundary scattering is considered. The relaxation time for the boundary scattering is given as

$$\left[\tau_b^{\mathrm{L(T)}}(L)\right]^{-1} = v_{\mathrm{L(T)}}/d,$$

where d is the effective scattering length for boundary scattering, which depends on the types of nanostructures involved. For the through-plane thermal conductivity of a thin film, $d = h$, where h is the thickness of the thin film. For the in-plane thermal conductivity of a thin film, $d = 2h$; the factor of 2 is a geometrical factor. For the thermal conductivity of an NW, $d = 2r$, where r is the diameter of the NW. For the thermal conductivity of crystals embedded with nanoparticles, $d = l_{\mathrm{Np}}$, where l_{Np} is the mean-free-path of phonons owing to scattering by nanoparticles according to the geometrical limit [23]. Although $\tau_b^{\mathrm{L(T)}}$ for nanostructures depends on group velocity and the value of effective diameter of the sample, L_{eff}, it is not independent of temperature or frequency [19]:

$$\left[\tau_b^{\mathrm{L(T)}}(L)\right]^{-1} = \frac{v_{\mathrm{L(T)}}}{L_{\mathrm{eff}}} = v_{\mathrm{L(T)}}\left(\frac{1}{L_C}+\frac{1}{L}\right) \tag{15}$$

where L is the length of the sample. For absolute temperature smaller than Debye temperature, the value of L_{eff} is on the order of cross-sectional dimensions, which is known as Casimir length (L_C). The relaxation rate of boundary scattering for longitudinal (transverse) mode is given by [3]

$$\left[\tau_b^{\mathrm{L(T)}}(L,\varepsilon)\right]^{-1} = v_{\mathrm{L(T)}}\left(\frac{1}{L_C}\frac{(1-\varepsilon)}{(1+\varepsilon)}+\frac{1}{L}\right). \tag{16}$$

Hence, $1/L_{\mathrm{eff}}$ is a specularity parameter, which depends on the frequency of phonon and the rate of surface roughness, ε. Surface roughness has a value in the range ($0 \le \varepsilon \le 1$), with the maximum value ($\varepsilon = 1$) representing complete phonon specular reflection and the minimum value ($\varepsilon = 0$) showing complete phonon diffuse surface scattering. In this work, for each InAs NW, the value of ε is determined by fitting the theoretical LTC with experimental data.

2.2d *Phonon–dislocation scattering rate*: For phonon–dislocation scattering, Nabarro separated the effects of the core from the surrounding strain field [27]. Crystals including dislocation (linear defect) undergo another phonon-scattering process. The corresponding relaxation rates are [28]

$$\left[\tau_{\mathrm{DC}}^{\mathrm{L(T)}}(x)\right]^{-1} = \eta N_D \frac{V_o^{4/3}}{v_{\mathrm{L(T)}}^2}\left(\frac{k_B T}{\hbar}\right)^3 x^3 \tag{17}$$

where $\eta = 55$ as in [26] and N_D is the number of dislocation lines per unit area. The values of dislocation density for each investigated specimen are listed in table 3.

2.2e *Phonon–electron scattering rate*: The concentration of free electrons in semiconductors increases with increased temperature and the doping process in semiconductors. Electrons can scatter phonons, so at low doping levels, the

Table 3. Fitting parameters of InAs NWs used in this work to calculate the LTCs of NW with different diameters.

Diameter (nm)	$N_{imp} \times 10^{26}$ (m^{-3})	$N_D \times 10^{14}$ (m^{-2})	$n_e \times 10^{26}$ (m^{-3})	ε	L_C (nm)	Sample length L (m)	γ_L	γ_T
Bulk	0.3	1.15	0.0085	0	2.24×10^6	2×10^{-3}	1.8	0.88
148	0.004	1.15	0.4	0.15	148	4×10^{-6}	1.99	0.89
100	0.045	1.16	0.5	0.6	100	4×10^{-6}	2	0.9
66	0.1	1.17	3.0	0.72	66	4×10^{-6}	2.58	0.94
63	0.3	1.18	6.3	0.97	63	4×10^{-6}	2.62	0.98
50	2.5	1.2	26	0.99	50	4×10^{-6}	2.7	0.99

relaxation time for acoustic phonons scattered by electrons can be expressed as [29]

$$\left[\tau_{ph-e}^{L(T)}(x)\right]^{-1} = \frac{n_e E^2 x}{\rho v_{L(T)}^2 \hbar}\sqrt{\frac{\pi m^* v_{L(T)}^2}{2k_B T}}\exp\left(-\frac{m^* v_{L(T)}^2}{2k_B T}\right) \tag{18}$$

where n_e is the electron-concentration density, E is the deformation potential and ρ is the mass density. The quantitative value for each mentioned parameter is given in table 3.

2.3 *LTC in NWs*

To calculate LTC for NWs, modifications of the bulk formula have to be made, including size-dependent parameters. The effects of acoustic phonon confinement and boundary scattering caused by non-equilibrium phonon distribution should also be considered [29]. Two factors affecting phonon confinement are phonon dispersion and acoustic group velocity. The value of phonon group velocity decreases with decreasing nanostructure size because of quantum effect on the surface of nanostructures [17,18,29]. Zou and Balandin [29] showed the role of phonon confinement in decreasing the LTC of nanostructures. The theoretical model for LTC calculation is well fitted with the experimental data [3,24,34] after considering the size-dependent physical parameters [30].

In the present work, each impurity density N_{imp}, surface roughness ε, carrier concentration n_e, Grüneisen parameter γ and lattice dislocation density N_D are determined from the fitting parameters, and their quantities are listed in table 2. Moreover, the following size-dependent parameters are calculated (as shown in table 1): mean bond length d_{mean}, melting temperature T_m, vibrational entropy S_{vib}, enthalpy of melting H_m, lattice parameter a and lattice volume V.

Two more quantities that split the Callaway model into longitudinal and transverse modes are phonon group velocity and Debye temperature. Phonon group velocity can be calculated for each mode of NW materials [20]. Similarly, Debye temperature as a function of phonon group velocity and zone-boundary phonon frequency can be calculated for the longitudinal and transverse modes of the bulk materials [14].

2.3a *Mean bond length*: The value of mean bond length starts to increase with decreasing crystal size to nanoscope, $d_{mean}(r)$, and this increment reaches the maximum value, $d_{mean}(r_c)$, when the nanostructure size material reaches a critical size, r_c. The change in mean bond length for semiconductors can be calculated as follows [30]:

$$\Delta d_{mean}(r) = \Delta d_{mean}(r_c)\left[\exp\left(\frac{-2(S_m(\infty) - R)}{3R\left(\frac{r}{r_c} - 1\right)}\right)\right]^{1/2} \tag{19}$$

where R is the ideal gas constant, r_c depends on the dimension of nanostructure materials ($r_c = [3 - D]h$, where D is dimension, which for quantum dots, NW and nanolayer is equal to zero, one and two, respectively), and h is the first solid surface layer height, which can be calculated as [30]

$$h = 1.429\, d_{mean}(\infty). \tag{20}$$

In equation (19), S_m is the vibrational entropy for bulk and can be calculated as follows:

$$S_m(\infty) = H_m(\infty)/T_m \tag{21}$$

where $H_m(\infty)$ is the enthalpy of melting, which is a function of bulk melting temperature:

$$H_m(\infty) = -10^{-5}\, T_m^2(\infty) + 0.059\, T_m(\infty) - 21.33. \tag{22}$$

Mean bond length as a function of size is given by [35]

$$d_{mean}(r) = h - \Delta d_{mean}(r). \tag{23}$$

Furthermore, the bulk value of d_{mean} can be determined as follows:

$$d_{mean}(\infty) = h - \Delta d_{mean}(r_c). \tag{24}$$

2.3b *Lattice constant and lattice volume*: The physical dimensions representing the unit cell of a crystal lattice is the lattice constant, whose quantity can be calculated as follows [36]:

$$a(r) = \frac{4}{\sqrt{3}} d_{\text{mean}}(r). \tag{25}$$

Thus, lattice volume is calculated from the relation [2]

$$V(r) = \left[\frac{a(r)}{2}\right]^3. \tag{26}$$

2.3c *Melting temperature*: For semiconductor materials, melting temperature as a function of size is given by [35]

$$\frac{T_{\text{m}}(r)}{T_{\text{m}}(\infty)} = \left(\frac{V(r)}{V(\infty)}\right)^{2/3} \exp\left[-\frac{2(S_{\text{m}}(\infty) - R)}{3R\left(\frac{r}{r_{\text{c}}} - 1\right)}\right]. \tag{27}$$

Given that lattice volume for nanostructure semiconductors increases with deceasing size, then according to equation (27), the melting temperature should also decrease.

2.3d *Debye temperature and lattice group velocity*: When nanosized materials are in consideration, Debye temperature can be calculated by Lindmann's formula [37,38]:

$$\left(\frac{\theta_{\text{D}}^{\text{n}}}{\theta_{\text{D}}^{\text{B}}}\right)^2 = \frac{T_{\text{m}}^{\text{n}}}{T_{\text{m}}^{\text{B}}}. \tag{28}$$

In addition, the result of Debye temperature obtained from equation (28) can be used to express a relationship for lattice group velocity. This parameter is extracted from [39] based on the assumption of an isotropic system and is given by

$$\frac{v^{\text{n}}}{v^{\text{B}}} = \frac{\theta_{\text{D}}^{\text{n}}}{\theta_{\text{D}}^{\text{B}}}. \tag{29}$$

The basic parameters for InAs are listed in table 1. The outcomes of the calculations for InAs NWs (with diameters of 50, 63, 66, 100 and 148 nm) are listed in table 3.

3. Results and discussion

3.1 *LTC in bulk InAs*

Figure 1 shows the experimentally measured and theoretically calculated LTC spectra for the bulk state of InAs at various temperatures. The curves include high-, intermediate- and low-temperature regions. In the low-temperature range ($T < 10$ K), LTC is governed by phonon scattering on the crystal surface known as boundary scattering. In this region, thermal conductivity is proportional to T^3 and it varies linearly with the sample dimension when surface scattering is strictly within the Casimir length [40]. For a circular cylinder shape with radius R, this length is equal to $L_{\text{C}} = 2R$, whereas for a square or rectangular cross-section with side lengths $L_{\text{C}} = 1.12L$, the length of the sample (L) is equal to 2 mm. The Casimir length (L_{C}) is determined from the cross-section of the sample, i.e., $L_{\text{C}} = 2.24 \times 10^6$ nm. The theoretical calculation agrees well with the experimental data, especially in the low-temperature region of up to 90 K (see extracted parameters in table 1). To achieve the best fitting of the calculated LTC curve to that of the experimental one, some parameters have to be carefully adjusted. Utilizing equations (28 and 29), the longitudinal and transverse Debye temperatures and acoustic group velocities for InAs NWs are calculated and are listed in table 1.

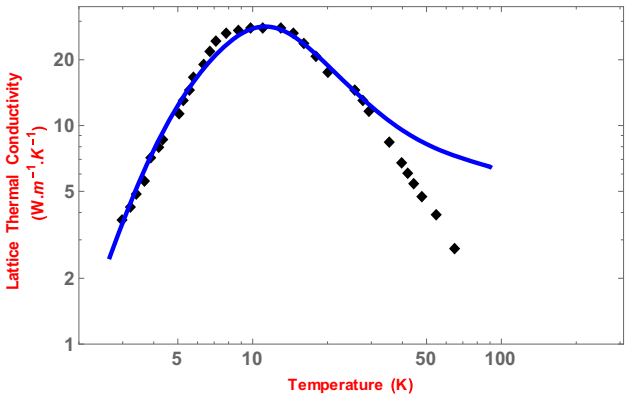

Figure 1. Lattice thermal conductivity of InAs bulk as a function of temperature. The theoretical calculation (solid line) was fitted to the experimental data (filled rectangular) at high temperature and extended for low temperature. Experimental data for ZB InAs were extracted from ref. [41].

Based on the results shown in figure 1 and table 3, one can see that the best fitting is achieved at low and intermediate temperatures. However, the estimation of relative contributions of transverse and longitudinal phonons to the heat conductivity of InAs at high temperature depends on the scattering rates for phonon–phonon process. Nevertheless, this was unable to be conclusively established in the current work. Noticeably, in the temperature range of $T > 50$ K, the thermal conductivity sharply decreases, and no fits are possible on the basis of three-phonon processes alone.

3.2 *LTC of InAs NWs*

Figure 2 shows the fitted and experimental results of InAs NWs with different sizes (50, 63, 66, 100 and 148 nm) within 0–300 K. The calculated/fitted data were estimated based on the use of Callaway expression. At low temperature ($T < 50$ K), all LTCs are related to T^3. The maximum values of LTC and their corresponding temperature depend on the diameter of NWs. The quantitative values for each

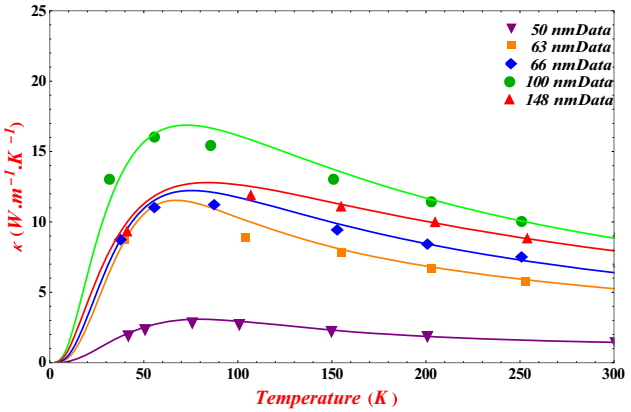

Figure 2. Calculated lattice thermal conductivities of InAs NWs for several diameters: WZ phases (50, 63, 66 and 100) nm and ZB phase (148 nm). The theoretical calculation (solid line) is fitted with experimental data from ref. [11]. ZB NWs are along the ⟨111⟩ direction and the WZ NWs are along *c*-axis.

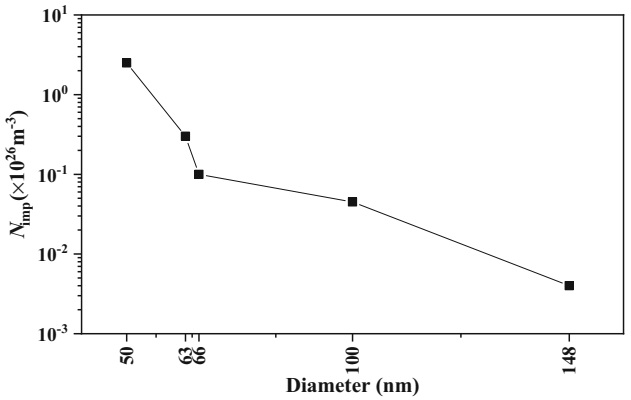

Figure 3. Impurity densities for diameters of 50, 63, 66, 100 and 148 nm are found for each InAs NW. The quantitative value increases with decreasing nanostructure size.

impurity, carrier concentration, surface roughness, Casimir length and Grüneisen parameters were not measured for InAs; hence, they were assumed to be adjustable parameters and determined using the fitting curves of LTC. The related experimental results are given in table 2.

Using equations (1)–(18), LTCs were calculated, which are size-dependent parameters; meanwhile, equations (19)–(29) were used for InAs NWs. The values for mean path length, lattice constant, unit-cell volume, melting temperature, longitudinal and transverse Debye temperatures and group velocity are listed in table 1. The shape of LTC is due to relaxation rates, i.e., LTCs are significantly affected by low-temperature boundary and phonon–electron scattering rate, by moderate-temperature impurity and dislocation relaxation rates, and by high-temperature Umklapp scattering.

Although size and temperature can influence the amount of thermal conductivity, the type of crystal structures such as

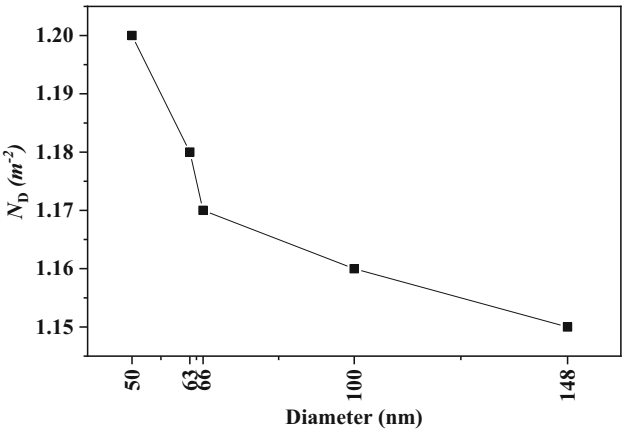

Figure 4. Dislocation densities for InAs with diameters of 50, 63, 66, 100 and 148 nm are handled in this work to fit theoretical results with experimental ones.

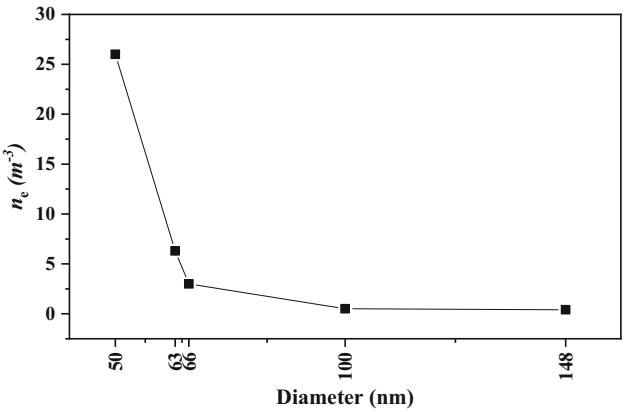

Figure 5. Carrier concentration as a function of diameter of InAs NWs used to fit the calculated LTCs in this work for diameters of 50, 63, 66, 100 and 148 nm.

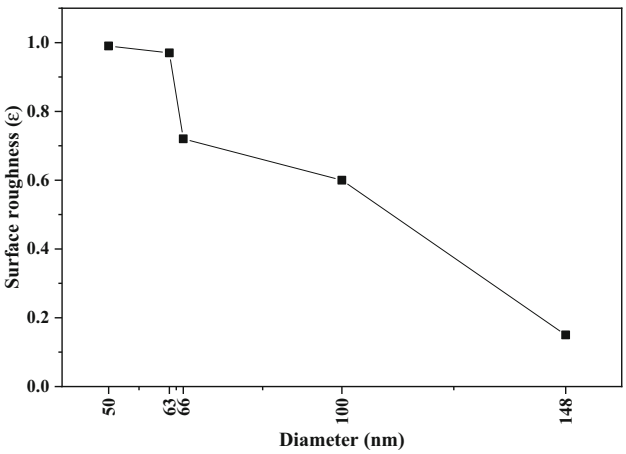

Figure 6. Surface roughness for InAs NWs with diameters of 50, 63, 66, 100 and 148 nm is used as a fitting parameter in this work.

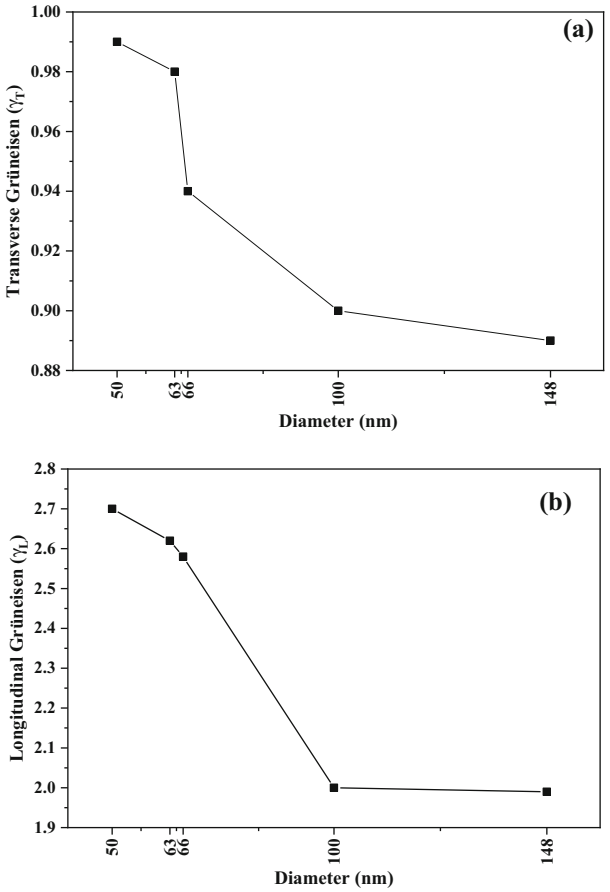

Figure 7. **(a)** Transverse and **(b)** longitudinal Grüneisen parameter as a function of the size that is used to fit theoretical LTCs with the corresponding experimental data of InAs NWs.

ZB and WZ plays an important factor in making the 100-nm diameter InAs NW to have higher LTC compared with that of 148 nm. Different values of LTC are observed for InAs NWs, which can be mainly due to different diameters and diffused surface scattering mean free paths [12].

The changes in fitting parameters according to the change in NW sizes are plotted as shown in figures 3–7. These parameters include impurity density, dislocation density, carrier concentration, surface roughness and Grüneisen parameter. Results show that all parameters decrease with increasing nanoscale size of InAs NWs.

4. Conclusions

The Morelli–Callaway model can be used to successfully calculate the thermal conductivity of InAs of the ZB and WZ phases in bulk and NW form. Calculations are executed for InAs NWs with diameters 50, 63, 66, 100 and 148 nm. Some parameters are calculated using size-dependent equations. For parameters such as mean free path, lattice parameter, unit-cell volume and acoustic group velocity, their quantitative values increase with decreased size of the sample InAs. However, the melting and Debye temperatures decrease with decreased NW size. Moreover, the values of dislocation, impurity, carrier concentration and surface roughness are found though the fitting curves, and their values increase with decreasing NW size.

However, the determination of the relative contributions of transverse and longitudinal phonons to the heat conductivity of InAs at high temperatures depends on the scattering rates selected from phonon–phonon processes, and results cannot be conclusively established. In general, LTC for a given temperature depends on the size and crystal structure of InAs nanoforms. At room temperature, the thermal conductivity of WZ bulk InAs is higher than those of all ZB InAs NWs mentioned in the current work.

Acknowledgements

Authors would like to thank Mr Ibrahim Nazem Qader from the College of Science, University of Raparin, for his help and assistance during our work. Authors also thank the College of Science, University of Salahaddin – Erbil for the financial support under Grant No. 7/54/2423.

References

[1] Morelli D T and Slack G A 2006 *High thermal conductivity materials* (New York: Springer, NP)
[2] Omar M and Taha H 2009 *Physica B: Condens. Matter* **404** 5203
[3] Omar M and Taha H 2010 *Sadhana* **35** 177
[4] Estreicher S, Gibbons T and Bebek M 2015 *J. Appl. Phys.* **117** 112801
[5] Cahill D G, Braun P V, Chen G, Clarke D R, Fan S H, Goodson K E *et al* 2014 *Appl. Phys. Rev.* **1** 011305
[6] Majumdar D, Basu A, Mukherjee G D, Ercolani D, Sorba L and Singha A 2014 *Nanotechnology* **25** 465704
[7] Madelung O 2012 *Semiconductors: data handbook* (New York: Springer, NP)
[8] Zhou F, Moore A L, Bolinsson J, Persson A, Froberg L, Pettes M L *et al* 2011 *Phys. Rev. B* **83** 205416
[9] Migunov V 2009 *Master thesis* (Universität Duisburg-Essen)
[10] Le Guillou G and Albany H 1972 *Phys. Rev. B* **5** 2301
[11] Li W and Mingo N 2013 *J. Appl. Phys.* **114** 183505
[12] Qader I N, Abdullah B J and Karim H H 2017 *Eurasian J. Sci. Eng.* **3** 9
[13] Shur M S 1996 *Handbook series on semiconductor parameters* (Singapore: WorldScientific, NP)
[14] Morelli D, Heremans J and Slack G 2002 *Phys. Rev. B* **66** 195304
[15] Callaway J 1959 *Phys. Rev.* **113** 1046
[16] Asen-Palmer M, Bartkowski K, Gmelin E and Cardona M 1997 *Phys. Rev. B* **56** 9431
[17] Balandin A and Wang K L 1998 *Phys. Rev. B* **58** 1544
[18] Khitun A, Balandin A and Wang K 1999 *Superlattice. Microst.* **26** 181
[19] Qader I N and Omar M 2017 *Bull. Mater. Sci.* **40** 599

[20] Hou H, Yang J, Hu F, Zhang S and Yang S 2014 *Chalcogenide Lett.* **11** 121
[21] Qader I N, Abdullah B J, Hassan M A and Mahmood P H 2019 *Eurasian J. Sci. Eng.* **4** 55
[22] Kazan M, Guisbiers G, Pereira S, Correia M R, Masri P, Bruyant A *et al* 2010 *J. Appl. Phys.* **107** 083503
[23] Koh Y K 2010 *Heat transport by phonons in crystalline materials and nanostructures* (Urbana-Champaign: University of Illinois)
[24] Mamand S, Omar M and Muhammad A 2012 *Mater. Res. Bull.* **47** 1264
[25] Tritt T M 2005 *Thermal conductivity: theory, properties, and applications* (New York: Springer, NP)
[26] Klemens P 1955 *Proc. Phys. Soc. A* **68** 1113
[27] Nabarro F 1951 *Proc. R. Soc. Lond. A* **209** 278
[28] Zou J 2010 *J. Appl. Phys.* **108** 034324
[29] Zou J and Balandin A 2001 *J. Appl. Phys.* **89** 2932
[30] Omar M 2016 *Int. J. Thermophys.* **37** 11
[31] de Laeter J R, Böhlke J K, De Bièvre P *et al* 2003 *Pure Appl. Chem.* **75** 683
[32] De Bievre P and Taylor P 1993 *Int. J. Mass Spectrom. Ion Processes* **123** 149
[33] Zou J, Kotchetkov D, Balandin A, Florescu D and Pollak F H 2002 *J. Appl. Phys.* **92** 2534
[34] Mamand S and Omar M 2014 *Adv. Mater. Res.* **832** 33
[35] Omar M 2012 *Mater. Res. Bull.* **47** 3518
[36] Omar M 2007 *Mater. Res. Bull.* **42** 319
[37] Liang L and Li B 2006 *Phys. Rev. B* **73** 153303
[38] Dash J 1999 *Rev. Mod. Phys.* **71** 1737
[39] Post E 1953 *Can. J. Phys.* **31** 112
[40] Wen Z, Zhao M and Jiang Q 2000 *J. Phys.: Condens. Matter* **12** 8819
[41] Swinkels M Y, van Delft M R, Oliveira D S, Cavalli A, Zardo I, van der Heijden R W *et al* 2015 *Nanotechnology* **26** 385401